ARTICLES

Time-Resolved Thermally Activated Delayed Fluorescence in C_{70} and 1,2-$C_{70}H_2$

Sergei M. Bachilo, Angelo F. Benedetto, R. Bruce Weisman,* Jamie R. Nossal, and W. Edward Billups

Department of Chemistry, Rice University, Houston, Texas 77251

Received: July 31, 2000; In Final Form: September 27, 2000

Thermally activated delayed fluorescence (TDF) emission from C_{70} and 1,2-$C_{70}H_2$ has been time-resolved to provide thermodynamic and kinetic information on excited electronic states. The energy gap between S_1 and T_1 states was deduced from the temperature dependence of initial TDF intensities and independently from the ratio of TDF intensity to time-integrated prompt fluorescence. S_1-T_1 gaps were found to be approximately 2470 cm^{-1} for C_{70} and 2180 cm^{-1} for 1,2-$C_{70}H_2$, with relative uncertainties of 2−3%. Time-resolved TDF measurements from fullerene samples immobilized in PMMA films revealed lifetimes for triplet state decay unaffected by bimolecular deactivation processes. The intrinsic triplet lifetimes at 298 K were found from both TDF and transient absorption measurements to be 24.5 ± 1.5 ms for C_{70} and 1.95 ± 0.1 ms for 1,2-$C_{70}H_2$.

Introduction

Following optical excitation, organic molecules in solution normally relax very quickly to S_1, the lowest-lying electronically excited singlet state. Subsequent depopulation of S_1 through radiative and nonradiative channels is reflected in the decay of $S_1 \rightarrow S_0$ fluorescence emission. Often, one of the most efficient nonradiative channels for S_1 depopulation is intersystem crossing to form T_1, the lowest triplet electronic state, the lifetime of which can greatly exceed the S_1 lifetime. If the energy gap between S_1 and T_1 is small, a portion of the triplet population formed in this process can become thermally re-excited to S_1, giving a weak, delayed fluorescence component with kinetics matching that of the triplet state. Such thermally activated delayed fluorescence (TDF) was observed by Boudin in 1930[1] and later elucidated by Parker and Hatchard.[2]

Many fullerenes have photophysical characteristics that make them suitable for TDF studies. C_{60} and C_{70} undergo $S_1 \rightarrow T_1$ intersystem crossing much more rapidly than they fluoresce or internally convert from S_1 to S_0, leading to quantum yields of triplet state formation near 1.0.[3−9] Once formed, these triplet states can live 5−7 orders of magnitude longer than the S_1 state.[10] The combination of long triplet lifetimes and modest S_1-T_1 energy gaps allows the total, time-integrated TDF to exceed the amount of prompt fluorescence. Berberan-Santos and co-workers have reported studies of such time-integrated TDF for C_{60} and C_{70}.[9,11]

TDF measurements on fullerenes can provide two types of important information. The first concerns the relative energies of the S_1 and T_1 states. Although in principle this energy gap may be obtained by subtracting the origin frequencies of fluorescence and phosphorescence spectra, the properties of fullerenes can make this approach difficult. Fullerene phosphorescence is often very weak, forbidden by symmetry as well as spin selection rules. Detector noise and impurity emissions may therefore obscure or distort the desired phosphorescence spectra, which fall at inconveniently long wavelengths. Even if these problems are absent, spectral broadening and complications such as false origins can differ between fluorescence and phosphorescence spectra, causing errors in S_1-T_1 gap determinations. By contrast, measurements of TDF intensity as a function of temperature can reveal the true thermodynamic (nonvertical) energy gap between the singlet and triplet electronic surfaces. However, for this purpose one should use time-resolved TDF signals, because the time-integrated TDF signals will contain an additional temperature dependence arising from variations in the triplet state lifetime. In addition, time-resolved fluorescence data at a single temperature may be analyzed for the ratio of initial TDF intensity to integrated prompt fluorescence to obtain a second, independent measure of the S_1-T_1 gap. TDF measurements therefore offer the benefit of redundant determination of singlet−triplet energy gaps.

The second type of information available from time-resolved TDF is triplet state population kinetics. Two alternative time-resolved methods are normally used to measure such triplet state kinetics: phosphorescence emission and induced absorption. For fullerenes, phosphorescence emission is difficult to time-resolve because of low intensities and near-infrared wavelengths. By contrast, TDF has the advantage of providing higher intensities (except at reduced temperatures) at more easily detected wavelengths. In some ways, time-resolved TDF is also preferable to induced absorption. As an emission method, it measures signals against a zero background instead of extracting small differences between large quantities. TDF measurements may therefore be made with relatively simple apparatus that does not require a probe beam. Another advantage of time-resolved TDF arises from the fact that fluorescence spectra are generally sharper than triplet−triplet spectra. For mixed samples in which

* Corresponding author. Fax: 713-348-5155. E-mail: weisman@rice.edu.

10.1021/jp002742k CCC: $19.00
Published on Web 11/10/2000

the component species have overlapping $T_n \leftarrow T_1$ spectra, TDF may therefore allow selective monitoring of a single species's triplet kinetics.

We report here the first measurements of time-resolved TDF from fullerenes. Our samples are C_{70} and its simplest derivative, 1,2-$C_{70}H_2$. In this "*a,b*-[6,6]-closed" adduct, hydrogens are bound to two adjacent carbon atoms at a junction of six-membered rings closest to the "pole" of the C_{70} molecule. Samples were dissolved in films of poly(methyl methacrylate) (PMMA) to suppress diffusional bimolecular processes and allow observation of purely unimolecular relaxation. Our time-resolved TDF data therefore provide values for intrinsic triplet state decay constants as well as for S_1-T_1 energy gaps. These results are validated by comparison to findings from triplet−triplet absorption measurements and emission spectroscopy.

Experimental Methods

The preparation and purification of the studied compounds have been described in our earlier report that compared the basic photophysical properties of C_{70} and its dihydride.[12] We prepared samples dissolved in polymer by mixing viscous toluene solutions of PMMA with solutions of fullerene. To obtain films approximately 200 μm thick, these mixtures were applied to glass substrates, evaporated in darkness for 1 day at ambient temperature, and then dried under vacuum for about 1 h. The absorption spectra of the resulting C_{70} and 1,2-$C_{70}H_2$ PMMA films were very similar to the corresponding spectra in fluid toluene. Samples on glass substrates were mounted in an optical cryostat (Oxford Optistat-DN), and the sample chamber was then evacuated and refilled with purified nitrogen gas. We used an Oxford temperature controller to select and stabilize the sample temperature within 1 K over the range from 77 to 325 K. Some experiments were also performed at room temperature with the samples held in a special vacuum cell. Steady-state absorption and fluorescence spectra were recorded using a Cary 4 spectrophotometer and a Spex Fluorolog 3-11 spectrofluorometer.

For measuring TDF and induced absorption, samples were excited by 532 nm nanosecond-scale pulses from a frequency-doubled Nd:YAG laser. The applied pulse energy did not exceed 2 mJ and the irradiated sample area ranged from 0.1 to 1 cm^2 in different measurements. We used a stabilized tungsten−halogen lamp to generate probing light for induced absorption measurements. An amplified silicon photodiode mounted after a computer-controlled grating monochromator (ISA Triax-180) detected sample emission or transmitted probe light, depending on the experiment. The detection electronics had a response time of 0.7 μs. Signals were digitized and averaged by a Tektronix TDS-430A oscilloscope and then transferred to a laboratory computer over a GPIB interface. This detection system had a sensitivity of approximately 3×10^6 V/W and a noise-equivalent power (after signal averaging less than 1000 traces) near 5×10^{-11} W. Its dynamic range of greater than 10^5 allowed us to measure the weak TDF traces that followed intense signals from prompt fluorescence. Although photon counting provides higher detection sensitivity, the photodiode-based system used here can record single-shot traces extending to milliseconds while providing spectral coverage into the near-infrared with sub-microsecond time resolution and very high dynamic range. These capabilities are well-suited to the study of time-resolved TDF.

In this project we used the detection system described above to make time-resolved measurements of probe beam intensity (for induced absorption), phosphorescence emission, and delayed fluorescence. Because prompt fluorescence decayed far faster than the detector response time, it gave traces matching the instrumental response function, which has an exponential decay time of 0.7 μs and an effective width of $\sim$1 μs (determined as the ratio of the area under the trace to its peak amplitude). The time-integrated prompt fluorescence intensity was easily monitored from the area under such traces.

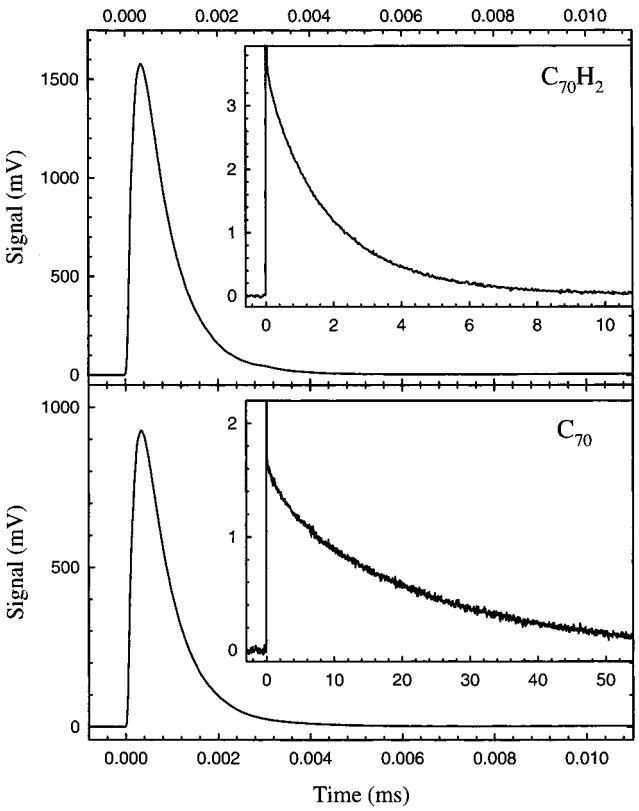

Figure 1. Kinetics of prompt and delayed emission of $C_{70}H_2$ (top frame, measured at 780 nm) and C_{70} (bottom frame, measured at 720 nm) in PMMA at 298 K. Because of the large differences in duration and intensity between the prompt and delayed signals, the weak long-lived parts are shown on separate scales in the inserts.

Results and Discussion

Kinetics of Thermally Activated Delayed Fluorescence. Figure 1 shows the emission kinetics recorded from our samples after pulsed excitation. The intense short-lived component was not time-resolved; instead, its apparent shape is the instrumental response function described above. We assign this fast emission signal to prompt fluorescence. Raman scattering, which would have the same apparent time profile, was undetectably weak for our PMMA film samples in the observed spectral region. The intensity of prompt fluorescence was high enough to allow easy measurement of spectral scans. The resulting emission spectra agreed closely with steady-state fluorescence spectra of samples in toluene solutions, as measured in our laboratory and reported in other studies.[12,13] Decreasing the sample temperature to 77 K sharpened the fluorescence spectra, especially for C_{70}. While the spectral shape and weights of different vibronic bands changed slightly upon cooling, the peaks corresponding to 0−0 transitions did not shift substantially over our temperature range of 77 to 320 K. A major part of the "hot band" emission detected at wavelengths shorter than the 0−0 position disappeared upon cooling.

The insets of Figure 1 show the slowly decaying emission components as a function of time on greatly expanded sensitivity

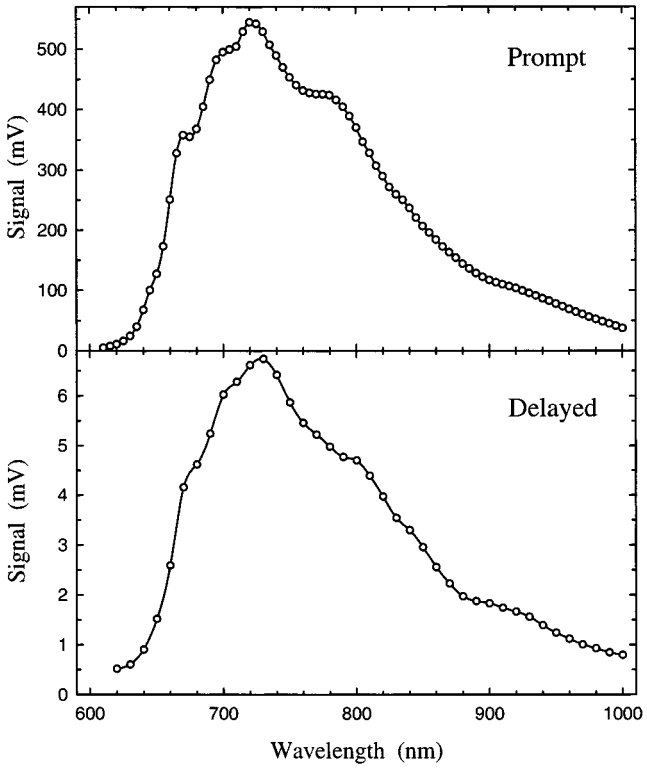

Figure 2. Spectra of the prompt and delayed emission components from C_{70} in PMMA at 298 K following pulsed excitation at 532 nm. These spectra are not corrected for the spectral sensitivity of the detection system.

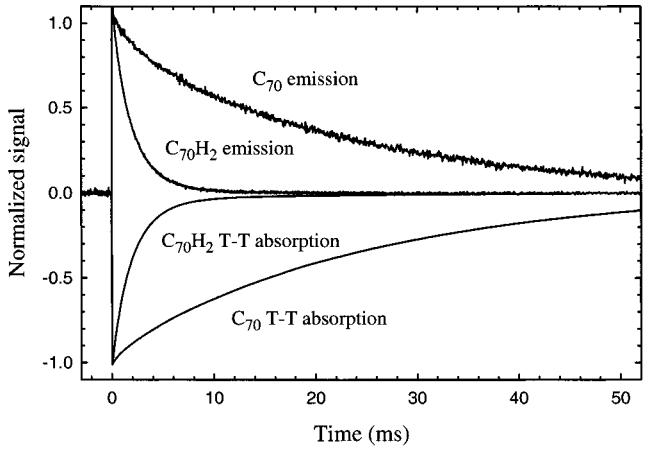

Figure 3. Kinetics of the delayed fluorescence (positive-going traces) and triplet−triplet absorption (negative-going traces) of C_{70} and 1,2-$C_{70}H_2$ in PMMA at 298 K. For comparison, all traces have been normalized to a peak amplitude of 1. Exponential lifetimes are 24.5 ± 1.5 ms for C_{70} and 1.95 ± 0.1 ms for 1,2-$C_{70}H_2$.

scales. Measured emission spectra of the prompt and delayed components are displayed in Figure 2 for C_{70}. The clear similarity of these two spectra indicates that the delayed emission is fluorescence rather than phosphorescence. In general, the source of delayed fluorescence may be either triplet−triplet annihilation (originally termed "P-type" delayed fluorescence)[14] or thermal activation of triplet states (TDF, originally termed "E-type" delayed fluorescence).[2] These processes can be distinguished kinetically, because TDF will match the triplet state population decay whereas emission from triplet−triplet annihilation will decay with twice that rate constant. Figure 3 compares the time-resolved delayed emission intensity from film

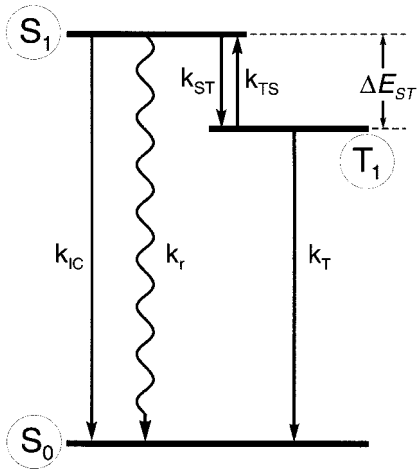

Figure 4. Jablonski diagram showing electronic states and kinetic processes relevant to the photophysical model discussed in the text.

samples of C_{70} and 1,2-$C_{70}H_2$ with $T_n \leftarrow T_1$ transient absorption data on the same samples. For clarity, the absorption traces are displayed as negative-going and all traces have been normalized to one. The obvious kinetic match between the delayed fluorescence and induced absorption data identifies the emission as TDF, as would be expected from the negligible diffusional mobility in PMMA films. We have found that fullerene samples show delayed fluorescence from triplet−triplet annihilation as well as from TDF when they are in fluid solvents.[15]

The decays of delayed emission and triplet absorption from our 1,2-$C_{70}H_2$ samples in PMMA can be accurately simulated by a first-order kinetic model. The 1.95 ± 0.1 ms exponential lifetime found at 298 K represents the intrinsic unimolecular lifetime of this derivatized fullerene against nonradiative $T_1 \rightarrow S_0$ decay. (The contribution from phosphorescence decay is negligible.) For C_{70} we sometimes found slightly nonexponential kinetics, an effect that may be related to minor sample inhomogeneity from the presence of tiny amounts of residual oxygen or other quenchers in the films. We note that because the analyses described in the following section are based on the initial amplitude of TDF instead of its time integral, they remain valid even for nonexponential triplet decay kinetics. The dominant triplet lifetime measured for C_{70} immobilized in PMMA at 298 K was 24.5 ± 1.5 ms, a value 12 times greater than that of 1,2-$C_{70}H_2$.

At lower temperatures, the TDF signal became weak enough that it was possible to record phosphorescence emission traces without interference. We found that the phosphorescence intensity showed only a mild dependence on temperature and was about 1 order of magnitude weaker than TDF at room temperature. The decay of phosphorescence emission matched the $T_n \leftarrow T_1$ induced absorption kinetics under corresponding conditions.

S_1−T_1 Energy Gap Determinations. Because TDF emission arises from thermal population of the singlet excited state, its intensity must show a characteristic temperature dependence that reveals the value of the S_1-T_1 energy gap.[16] We will use the symbol ΔE_{ST} to denote this gap, as illustrated by the simplified Jablonski diagram of Figure 4. This diagram also shows notations for unimolecular rate constants describing internal conversion and radiative decay from S_1, forward and reverse intersystem crossing between S_1 and T_1, and T_1 relaxation. The detected TDF intensity can be written as

$$I_f^{\text{delayed}}(t) = \alpha k_r [S_1]_t \qquad (1)$$

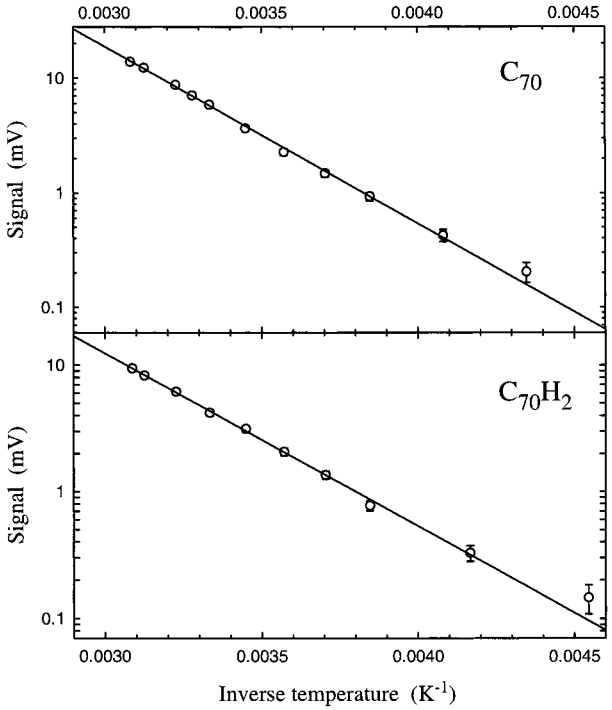

Figure 5. Temperature dependence of initial delayed fluorescence intensity from C_{70} (at 720 nm) and 1,2-$C_{70}H_2$ (at 780 nm). Solid lines show the fitting function $I_f^{delayed}(0) = I^0 \exp(-\Delta E_{ST}/k_BT)$ with parameters $I^0 = 803$ V, $\Delta E_{ST} = 2470$ cm^{-1} for C_{70}; and $I^0 = 154$ V, $\Delta E_{ST} = 2180$ cm^{-1} for $C_{70}H_2$.

where coefficient α represents detection sensitivity, k_r is the S_1 radiative rate constant, and $[S_1]_t$ is the concentration of molecules in S_1 at time t. After its initial nanosecond-scale decay, the S_1 concentration remains small because it is depleted much faster than it is formed by thermal excitation from T_1. We can then apply the steady-state approximation to obtain the following expression for $[S_1]_t$:

$$[S_1]_t = \frac{k_{TS}}{k_{IC} + k_r + k_{ST}}[T_1]_t \tag{2}$$

In addition, detailed balance provides the relation

$$\frac{k_{TS}}{k_{ST}} = \left(\frac{g_S}{g_T}\right)\exp\left(-\frac{\Delta E_{ST}}{k_BT}\right) \tag{3}$$

where g_S and g_T denote degeneracies of the S_1 and T_1 states and k_B is the Boltzmann constant. Combining eqs 2 and 3 gives

$$[S_1]_t = \frac{k_{ST}}{k_{IC} + k_r + k_{ST}}\left(\frac{g_S}{g_T}\right)\exp\left(-\frac{\Delta E_{ST}}{k_BT}\right)[T_1]_t \tag{4}$$

The first ratio in this expression equals Φ_T, the quantum yield for triplet formation. Equation 1 then becomes

$$I_f^{delayed}(t) = \alpha k_r \Phi_T\left(\frac{g_S}{g_T}\right)\exp\left(-\frac{\Delta E_{ST}}{k_BT}\right)[T_1]_t \tag{5}$$

This result applies to systems in which only the S_1 and T_1 excited states are photophysically active. Equation 5 predicts that the initial TDF intensity will show a simple Boltzmann-factor dependence on temperature if k_r, Φ_T, and g_S/g_T remain constant over the studied temperature range. In the case of C_{70} and 1,2-$C_{70}H_2$, the fluorescence intensity varies little over a wide temperature range and Φ_T is close to 1.0.[12] The degeneracy ratio can vary with temperature if the two electronic states have sufficiently different vibrational frequencies or if there are nearby excited states with significant thermal populations.

TABLE 1: Experimental Values for S_1-T_1 Energy Gaps (cm^{-1}) Found from Analysis of Emission Spectra and from TDF Measurements

	ΔE_{ST}			
compound	spectral peaks[a]	spectral edges[b]	TDF activation[c]	TDF intensity[d]
C_{70}	2450 ± 50	2580 ± 50	2470 ± 50	2575 (2485^e) ± 60
1,2-$C_{70}H_2$	2100 ± 60	2380 ± 90	2180 ± 60	

[a] Separation between the peaks of origin bands in fluorescence and phosphorescence spectra. [b] Separation between the half-maximum points on the high-frequency edges of fluorescence and phosphorescence origin bands. [c] From eq 6; the activation energy for temperature-dependent TDF intensities. [d] From eq 9 and the ratio of prompt to delayed fluorescence intensities at one sample temperature. [e] Using a corrected degeneracy ratio of 0.22, as described in the text.

Figure 5 shows the temperature dependence of initial TDF amplitudes for C_{70} and 1,2-$C_{70}H_2$. Delayed fluorescence from both compounds becomes too weak for our system to detect upon cooling below 220 K. As can be seen from the solid-line fits in Figure 5, the TDF amplitudes were well fit over nearly 2 orders of magnitude of intensity change by simple activation functions of the form

$$I_f^{delayed}(0) = I^0 \exp(-\Delta E_{ST}/k_BT) \tag{6}$$

This implies that k_r, Φ_T, and g_S/g_T are nearly constant from 225 to 325 K for these samples. The deduced values of ΔE_{ST} are 2470 ± 50 cm^{-1} for C_{70} and 2180 ± 60 cm^{-1} for 1,2-$C_{70}H_2$, as listed in Table 1.

Comparison of eqs 5 and 6 shows that the preexponential factor can be written as

$$I^0 = \alpha k_r \Phi_T\left(\frac{g_S}{g_T}\right)[T_1]_0 = \alpha k_r \Phi_T^2\left(\frac{g_S}{g_T}\right)[S_1]_0 \tag{7}$$

where $[S_1]_0$ is the total concentration of excited singlet states generated by pulsed excitation, and we have used the relation $\Phi_T = [T_1]_0/[S_1]_0$. The parameter I^0 is approximately the peak delayed fluorescence amplitude in the limit of infinitely high temperature. Note that at the time zero used to define $[T_1]_0$, the triplet concentration must be fully formed from S_1 but not yet significantly depleted by decay processes. Any delay between a few nanoseconds and many microseconds satisfies this requirement for the samples studied here.

The value of ΔE_{ST} can also be deduced from a comparison of the prompt and delayed fluorescence signals. Although our detector cannot resolve the time profile of the prompt fluorescence, it electronically integrates the fluorescence photocurrent within its response time. Therefore, the area under the prompt portion of the recorded emission trace measures

$$\int I_f^{prompt}(t)\,dt = \alpha k_r \int [S_1]_t\,dt = \alpha k_r [S_1]_0 \tau_S \tag{8}$$

where τ_S is the population lifetime of S_1, equal to $(k_{IC} + k_r + k_{ST})^{-1}$ in the model of Figure 4.

Combining eqs 5 and 8, and using the relationship $\Phi_T = [T_1]_0/[S_1]_0$, we obtain

$$\frac{I_f^{delayed}(0)}{\int I_f^{prompt}(t)\,dt} = \Phi_T^2\left(\frac{g_S}{g_T}\right)\frac{1}{\tau_S}\exp\left(-\frac{\Delta E_{ST}}{k_BT}\right) \tag{9}$$

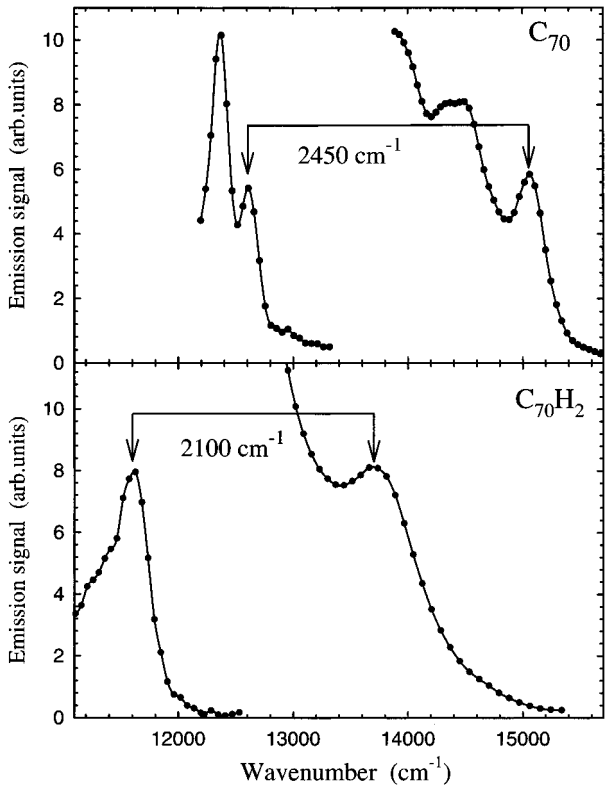

Figure 6. High-frequency portions of the corrected phosphorescence and fluorescence spectra for C_{70} at 200 K and 1,2-$C_{70}H_2$ at 140 K in PMMA, as used to determine the S_1-T_1 energy gaps.

If the values of Φ_T, g_S/g_T, and τ_S are known, then eq 9 allows one to deduce the value of ΔE_{ST} from a single-temperature measurement of a sample's fluorescence emission trace. We can apply this approach to C_{70}, for which reported values of Φ_T and τ_S are 1.0 and 0.7 ns, respectively. [9,15,17,18] In the absence of other information, one may assume that the ratio g_S/g_T is dominated by spin degeneracies and therefore equals $^1/_3$. The traces for C_{70} shown in Figure 1 give 1.70×10^{-3} V for $I_f^{delayed}(0)$ and 9.30×10^{-7} V s for $\int I_f^{prompt}(t)\, dt$. Using these values in eq 9, we find that ΔE_{ST} equals 2575 cm^{-1}, a result only 4% different from that obtained from the temperature dependence of TDF intensity. The g_S/g_T ratio used in evaluating eq 9 may be refined using prior results from this laboratory.[19] Temperature-dependent equilibrium constants were measured to find the relative entropies of triplet state fullerenes, and the orbital entropy of triplet state C_{70} was deduced to be 0.42 ± 0.05 R.[19] This value implies an effective orbital degeneracy of 1.52, apparently reflecting significant thermal population of a low-lying, doubly degenerate T_2 state. By combining this triplet state effective orbital degeneracy with the normal spin degeneracy of 3, one obtains a g_T value of 4.57 for C_{70}, which reduces the g_S/g_T ratio to 0.22. Reevaluation of eq 9 then gives $\Delta E_{ST} = 2485$ cm^{-1}, in excellent agreement with the thermal activation value of 2470 cm^{-1}. Our results for ΔE_{ST} of C_{70} are approximately 14% higher than the 2175 ± 170 cm^{-1} value reported by Berberan-Santos and Garcia from their time-integrated TDF study.[9]

To compare the TDF ΔE_{ST} findings with spectroscopic values, we have recorded the steady-state fluorescence and phosphorescence emission spectra of C_{70} and 1,2-$C_{70}H_2$. Figure 6 shows these spectra, with arrows marking the apparent vibronic origin peaks. The separation between these peaks, which should equal ΔE_{ST}, is listed in Table 1 along with ΔE_{ST} values found as the separations between the 50% intensity points on the high-frequency edges of those peaks. Because the broadening differs between the phosphorescence and fluorescence spectra, different values of ΔE_{ST} were obtained using these two analysis methods. For each sample, the ΔE_{ST} results from our TDF data fall between the two values determined from spectral analysis.

Conclusions

We have demonstrated that the time-resolved study of thermally activated delayed fluorescence (TDF) emission can provide both thermodynamic and kinetic information on fullerene excited electronic states. The nonvertical, thermodynamic energy gap between S_1 and T_1 states can be deduced from the temperature dependence of TDF intensities with a relative uncertainty near 2%. If the sample's prompt fluorescence lifetime and triplet quantum yield are known, then an independent estimate of the S_1-T_1 energy gap can easily be obtained from the ratio of TDF intensity to integrated prompt fluorescence at a single temperature. For some compounds, weak transitions or inaccessible wavelengths may prevent the T_1 energy from being directly measured by absorption or emission spectroscopy. In such cases, the T_1 energy can be reliably found by deducing the S_1-T_1 energy gap from TDF data and subtracting that result from the spectroscopically determined S_1 origin. Time-resolved TDF also provides a practical method for measuring fullerene triplet state kinetics while avoiding some of the difficulties of transient absorption methods.

Acknowledgment. We are grateful to the National Science Foundation and the Robert A. Welch Foundation for support of this research.

References and Notes

(1) Boudin, S. *J. Chim. Phys.* **1930**, *27*, 285.
(2) Parker, C. A.; Hatchard, C. G. *Trans. Faraday Soc.* **1961**, *57*, 1894.
(3) Arbogast, J. W.; Darmanyan, A. P.; Foote, C. S.; Rubin, Y.; Diederich, F. N.; Alvarez, M. M.; Anz, S. J.; Whetten, R. L. *J. Phys. Chem.* **1991**, *95*, 11.
(4) Terazima, M.; Hirota, N.; Shinohara, H.; Saito, Y. *J. Phys. Chem.* **1991**, *95*, 9080.
(5) Biczok, L.; Linschitz, H.; Walter, R. I. *Chem. Phys. Lett.* **1992**, *195*, 339.
(6) Bensasson, R. V.; Hill, T.; Lambert, C.; Land, E. J.; Leach, S.; Truscott, T. G. *Chem. Phys. Lett.* **1993**, *201*, 326.
(7) Arbogast, J. W.; Foote, C. S. *J. Am. Chem. Soc.* **1991**, *113*, 8886.
(8) Bensasson, R. V.; Hill, T.; Lambert, C.; Land, E. J.; Leach, S.; Truscott, T. G. *Chem. Phys. Lett.* **1993**, *206*, 197.
(9) Berberan-Santos, M. N.; Garcia, J. M. M. *J. Am. Chem. Soc.* **1996**, *118*, 9391.
(10) Weisman, R. B. Optical studies of fullerene triplet states In *Optical and Electronic Properties of Fullerenes and Fullerene-Based Materials*; Shinar, J., Vardeny, Z. V., Kafafi, Z. H., Eds.; Marcel Dekker: New York, 2000; pp 83−117.
(11) Salazar, F. A.; Fedorov, A.; Berberan-Santos, M. N. *Chem. Phys. Lett.* **1997**, *271*, 361.
(12) Benedetto, A. F.; Bachilo, S. M.; Weisman, R. B.; Nossal, J. R.; Billups, W. E. *J. Phys. Chem. A* **1999**, *103*, 10842.
(13) Sun, Y. P.; Bunker, C. E. *J. Phys. Chem.* **1993**, *97*, 6770.
(14) Parker, C. A.; Hatchard, C. G. *Trans. Faraday Soc.* **1963**, *59*, 284.
(15) Bachilo, S. M.; Weisman, R. B. *J. Phys. Chem. A* **2000**, *104*, 7711.
(16) Parker, C. A. *Photoluminescence of Solutions*; Elsevier: Amsterdam, 1968.
(17) Tanigaki, K.; Ebbesen, T. W.; Kuroshima, S. *Chem. Phys. Lett.* **1991**, *185*, 189.
(18) Kim, D.; Lee, M.; Suh, Y. D.; Kim, S. K. *J. Am. Chem. Soc.* **1992**, *114*, 4429.
(19) Ausman, K. D.; Weisman, R. B. *J. Am. Chem. Soc.* **1999**, *121*, 1110.